Roberts-Crowley and Rittenhouse
BMC Res Notes (2018) 11:681
https://doi.org/10.1186/s13104-018-3783-x

BMC Research Notes

RESEARCH NOTE

Open Access

Modulation of $Ca_V1.3b$ L-type calcium channels by M_1 muscarinic receptors varies with $Ca_V\beta$ subunit expression

Mandy L. Roberts-Crowley[1] and Ann R. Rittenhouse[1,2*]

Abstract

Objectives: We examined whether two G protein-coupled receptors (GPCRs), muscarinic M_1 receptors (M_1Rs) and dopaminergic D_2 receptors (D_2Rs), utilize endogenously released fatty acid to inhibit L-type Ca^{2+} channels, $Ca_V1.3$. HEK-293 cells, stably transfected with M_1Rs, were used to transiently transfect D_2Rs and $Ca_V1.3b$ with different $Ca_V\beta$-subunits, allowing for whole-cell current measurement from a pure channel population.

Results: M_1R activation with Oxotremorine-M inhibited currents from $Ca_V1.3b$ coexpressed with $\alpha_2\delta$-1 and a β_{1b}, β_{2a}, β_3, or β_4-subunit. Surprisingly, the magnitude of inhibition was less with β_{2a} than with other $Ca_V\beta$-subunits. Normalizing currents revealed kinetic changes after modulation with β_{1b}, β_3, or β_4, but not β_{2a}-containing channels. We then examined if D_2Rs modulate $Ca_V1.3b$ when expressed with different $Ca_V\beta$-subunits. Stimulation with quinpirole produced little inhibition or kinetic changes for $Ca_V1.3b$ coexpressed with β_{2a} or β_3. However, quinpirole inhibited N-type Ca^{2+} currents in a concentration-dependent manner, indicating functional expression of D_2Rs. N-current inhibition by quinpirole was voltage-dependent and independent of phospholipase A_2 (PLA_2), whereas a PLA_2 antagonist abolished M_1R-mediated N-current inhibition. These findings highlight the specific regulation of Ca^{2+} channels by different GPCRs. Moreover, tissue-specific and/or cellular localization of $Ca_V1.3b$ with different $Ca_V\beta$-subunits could fine tune the response of Ca^{2+} influx following GPCR activation.

Keywords: Acetylcholine, $Ca_V\beta$ subunit, Dopamine, L-type calcium current

Introduction

Voltage-gated Ca^{2+} channels (VGCCs) control membrane excitability, gene expression, and neurotransmitter release [1]. Alterations in these cellular functions occur when GPCR-activated signal transduction cascades modulate VGCCs. In medium spiny neurons (MSNs) of the striatum, GPCRs, including M_1Rs and D_2Rs, inhibit VGCC activity [2, 3]. These GPCRs specifically inhibit $Ca_V1.3$ L-current, decreasing the output of MSNs [3, 4] and may have functional consequences for motor control [5, 6].

Although present in MSNs, M_1R signaling has been characterized most thoroughly in superior cervical ganglion (SCG) neurons. M_1Rs couple to $G\alpha_q$ and phospholipase C (PLC) to inhibit native L- and N-VGCC currents [7–9]. This signal transduction cascade, referred to as the slow or diffusible second messenger pathway, is characterized as pertussis toxin (PTX)-insensitive, voltage-independent, and requiring intracellular Ca^{2+} to function [10]. Our laboratory has identified arachidonic acid (AA) as a critical effector in the slow pathway [9]. Exogenously applied AA inhibits L-current [11–13], which in SCG neurons most likely arises from $Ca_V1.3$ [14]. Moreover, Ca^{2+}-dependent cytosolic phospholipase A_2 ($cPLA_2$) appears critical for release of AA from phospholipids following M_1R activation; loss of $cPLA_2$ activity by pharmacological antagonists or gene knockout ablates L-current inhibition [15, 16].

*Correspondence: Ann.Rittenhouse@umassmed.edu
[2] Department of Microbiology and Physiological Systems, Program in Neuroscience, University of Massachusetts Medical School, 368 Plantation Street, Worcester, MA 01605, USA
Full list of author information is available at the end of the article

Additionally, D_2Rs inhibit L-current via a diffusible second messenger pathway involving phospholipase C (PLC), $InsP_3$, and calcineurin in MSNs [3]. While both GPCRs signal through PLC, they share another commonality: their activation releases AA from striatal neurons [17, 18] and transfected cell lines [19, 20]. Therefore, D_2Rs may also inhibit L- ($Ca_V1.3$) and N-($Ca_V2.2$) currents via a pathway utilizing $cPLA_2$ to release AA. In the present study, we tested whether the M_1R and D_2R pathways converge to modulate recombinant L-VGCC activity.

Main text

Materials and methods

Cell culture

Human embryonic kidney cells, stably transfected with the M1 muscarinic receptor (HEK-M1) [a generous gift from Emily Liman, University of Southern California, originally transfected by [21]] were propagated at 37 °C with 5% CO_2 in Dulbecco's MEM (DMEM)/F12 supplemented with 10% FBS, 1% G418, 0.1% gentamicin, and 1% HT supplement (Gibco Life Technologies). Cells were passaged when 80% confluent.

Transfection

HEK-M1 cells, grown in 12-well plates (~60–80% confluent), were transfected with a 1:1:1 molar ratio of $Ca_V1.3b$ or $Ca_V2.2$, $\alpha_2\delta$-1 and different $Ca_V\beta$s [22], using Lipofectamine PLUS (Invitrogen) according to the manufacturer's instructions. Cells were co-transfected with green fluorescent protein (GFP) to identify transfected cells. Constructs for $Ca_V1.3b$ (+exon11, Δexon32, +exon42a; GenBank accession #AF370009), $Ca_V2.2$ (^{a}10, Δexon18a, Δexon24a, +exon31a, +exon37b, +exon46; #AF055477), $Ca_V\beta_3$ (#M88751) and $\alpha_2\delta$-1 (#AF286488) were provided by Diane Lipscombe (Brown University). $Ca_V\beta_{1b}$ (#X61394), $Ca_V\beta_{2a}$ (#M80545), and $Ca_V\beta_4$ (#L02315) constructs were provided by Edward Perez-Reyes (University of Virginia). The $D_{4.4}$R (#AF1199329) construct was provided by Hubert H. M. Van Tol (University of Toronto). D_2R cDNA (#NM_000795) was obtained from the UMR cDNA Resource Center (https://www.cdna.org). Per well, a total of 0.5 µg of DNA (of which GFP cDNA was less than 10%) was used following the methods of Roberts-Crowley and Rittenhouse (2009) [13].

Electrophysiology

Whole-cell currents were recorded following the methods of Liu et al. [11]. High resistance seals were established in Mg^{2+} Tyrode's (in mM): 5 $MgCl_2$, 145 NaCl, 5.4 KCl, and 10 HEPES, brought to pH 7.50 with NaOH. Once a seal was established and the membrane ruptured, the Tyrode's solution was exchanged for external bath solution (in mM): 125 NMG-aspartate, 20 Ba-acetate, 10 HEPES, brought to pH 7.50 with CsOH. Only cells with ≥ 0.2 nA of current were used. Data were acquired using Signal 2.14 software (CED) and stored for later analysis on a personal computer. Linear leak and capacitive currents were subtracted from all traces.

Drugs

All chemicals were purchased from Sigma unless otherwise noted. FPL 64176 (FPL), nimodipine (NIM), and oleoyloxyethyl phosphorylcholine (OPC, Calbiochem) were prepared as stock solutions in 100% ethanol. Quinpirole (quin) and Oxotremorine-M (Oxo-M, Tocris) were dissolved in DDW and stored as 10 mM stock solutions at −70 °C. Stocks were diluted daily to the final concentration by at least 1000-fold with external solution. For ethanol-prepared stocks, the final ethanol concentration was less than 0.1%.

Statistical analysis

Data are presented as the mean ± s.e.m. Data were analyzed for significance using a Student's paired *t*-test for two means, or a one-way ANOVA followed by a Tukey multiple-comparison post hoc test. Statistical significance was set at $p < 0.05$ or < 0.001. Analysis programs included Signal (CED), Excel (Microsoft), and Origin (OriginLab).

Results

Characterization of recombinant $Ca_V1.3$ current as L-type in HEK-M1 cells

Whole-cell L-currents, from β_3-containing L-channels, elicited from a holding potential of −60 mV to a test potential of −10 mV, averaged −4699 ± 279 pA (n = 3) compared to −9 ± 1 pA for HEK-M1 cells transfected with only accessory subunits (n = 10, $P < 0.001$). Lack of current from cells transfected without $Ca_V1.3b$, confirmed that HEK-M1 cells exhibit little endogenous Ca^{2+} current and transfection of accessory subunits does not upregulate endogenous Ca^{2+} channels. Recombinant current was confirmed as L-type by showing sensitivity to the L-VGCC antagonist NIM. NIM inhibited β_3-containing currents (Additional file 1A) in a concentration-dependent manner (Additional file 1B). Currents were also sensitive to FPL, which enhanced current from β_{2a}- and β_3-containing channels and produced long-lasting tail currents upon repolarization (Additional file 1C, D). Additionally, FPL produced a slight hyperpolarizing voltage shift in the peak inward current and enhanced current amplitude at all voltages (Additional file 1E). Additional file 1F demonstrates that FPL enhanced the long-lasting tail current in a concentration-dependent manner. These pharmacological and biophysical

properties show that transfection of HEK-M1 cells with $Ca_V1.3b$ and accessory subunits produce currents with L-type characteristics.

The Ca_Vβ-subunit varies the magnitude of $Ca_V1.3$ current inhibition by M_1Rs

In MSNs, M_1R stimulation inhibits L-current in $Ca_V1.2$ knockout animals [4]. Only $Ca_V1.2$ and $Ca_V1.3$ constitute the L-type $Ca_V\alpha_1$ subunits expressed in brain [23], implying that M_1Rs specifically inhibit $Ca_V1.3$ current. Using a cell line transfected with only $Ca_V1.3$ channels provides molecular proof for the identity of the inhibited channel. Therefore, to determine if activation of M_1Rs inhibits $Ca_V1.3$ activity, peak current amplitudes were measured prior to and following application of the M_1R agonist Oxo-M. Figure 1a compares representative current traces for $Ca_V1.3b$ coexpressed with β_{1b}, β_{2a}, β_3, or β_4-subunits in the absence or presence of Oxo-M.

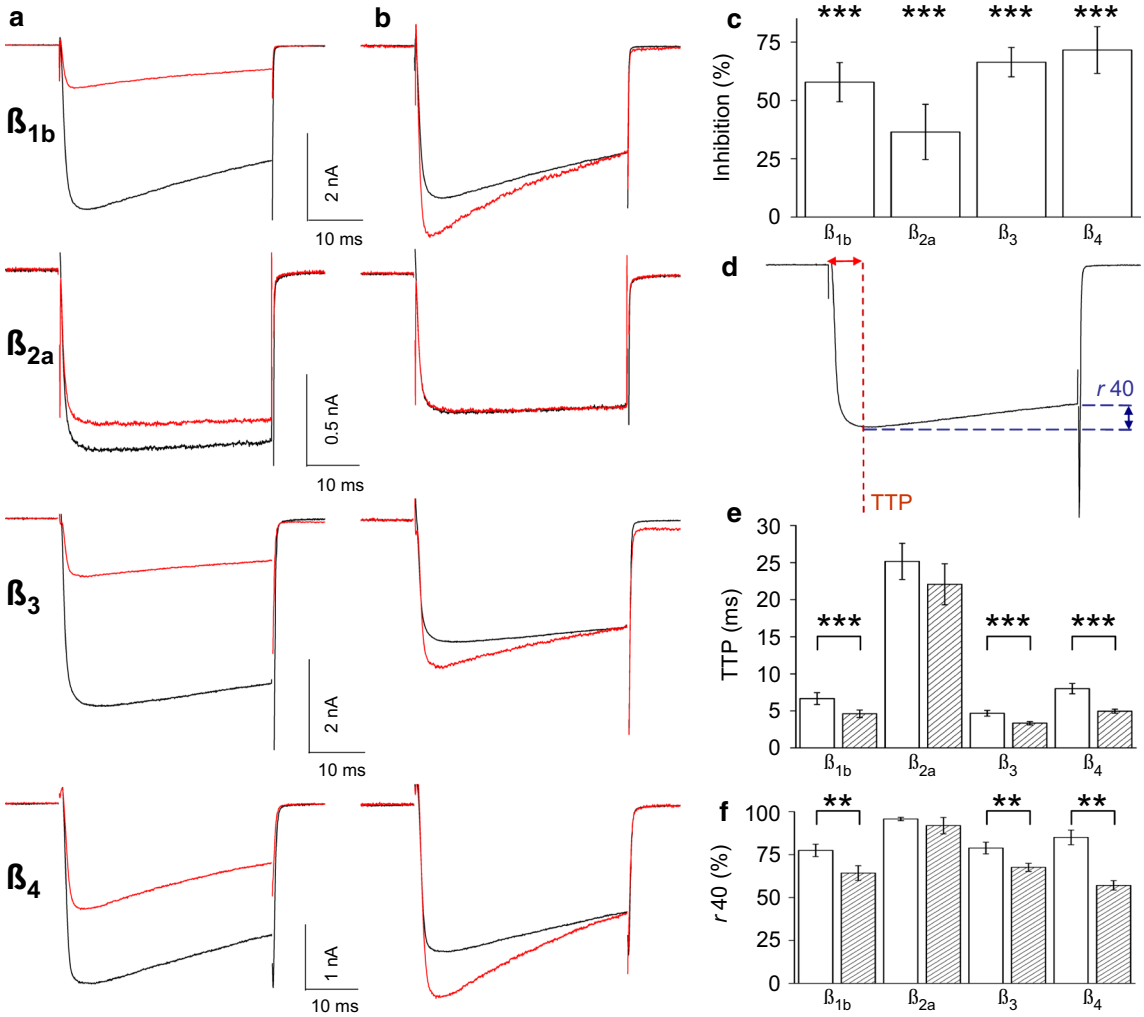

Fig. 1 $Ca_V1.3b$ current inhibition and kinetic changes produced by M_1R stimulation are Ca_Vβ-subunit dependent. **a** Representative current traces from $Ca_V1.3b$ coexpressed with β_{1b}, β_{2a}, β_3 or β_4 before (black) or 1 min after applying 10 μM Oxo-M (red). **b** Current traces from **a** were normalized to the end of the test pulse. **c** Summary of Oxo-M inhibition of $Ca_V1.3b$ with different Ca_Vβ-subunits. Maximal inward current amplitudes were measured after the onset of the test pulse using a trough seeking function (peak current). Percent of current inhibition was calculated as: $\%I_{inhib} = 100*(I_{CTL}-I_{DRUG})/I_{CTL}$, where I_{CTL} and I_{DRUG} are the average maximum current amplitude of 5 traces prior to and after 1 min of application of test material (unless otherwise noted). **d** Schematic of quantification of kinetic changes. **e**, **f** Summary of kinetic changes (n = 4–6, $^{***}P < 0.001$, $^{**}P < 0.05$) open bars, control; hatched bars, Oxo-M. **e** Time to peak (TTP) was measured using a minimum seeking function in Signal within the test pulse duration. **f** Current remaining (*r*40) was measured from an average of five normalized current traces per condition using the equation: $r40 = 100*I_{end}/I_{peak}$, where *r*40 is the percent of the maximum inward current remaining at the end of a 40 ms test pulse; I_{end} is the current amplitude at the end of the test pulse; I_{peak} is the maximum inward current measured during the test pulse

After 1 min, Oxo-M significantly inhibited L-current by 58 ± 8% with β_{1b}; 36 ± 12% with β_{2a}; 66 ± 6% with β_3; and 72 ± 10% with β_4 (Fig. 1c). Oxo-M elicited kinetic changes that were visualized by normalizing individual traces to the end of the 40 ms test pulse (Fig. 1b), which were quantified by measuring TTP and *r*40 (Fig. 1d). TTP (Fig. 1e) and *r*40 (Fig. 1f) decreased following Oxo-M with β_{1b}, β_3, or β_4; however, no changes were detected with β_{2a} ($P \geq 0.11$ for TTP; $P \geq 0.40$ for *r*40). These differences in the magnitude of current inhibition and kinetics suggest that the $Ca_V\beta$-subunit affects M_1R modulation of $Ca_V1.3b$.

Dopamine D_2 receptors inhibit $Ca_V2.2$ but not $Ca_V1.3$ currents

Both M_1Rs and D_2Rs activate pathways involving G proteins, PLC, and AA release (Fig. 2a). However, whether L-current inhibition by D_2Rs shows varied inhibition depending on $Ca_V\beta$-subunit expression has not been examined. Therefore, we coexpressed D_2Rs with $Ca_V1.3b$, $\alpha_2\delta$-1 and different $Ca_V\beta$-subunits. While Oxo-M inhibited $Ca_V1.3b$-β_{2a} currents over time (Fig. 2b), quin, a D_2R agonist, had no effect on current amplitude (Fig. 2c) or kinetics (Fig. 2c inset, g). Since $Ca_V1.3b$-β_{2a} current shows less inhibition and no kinetic changes with Oxo-M, we tested whether $Ca_V1.3b$-β_3 current was sensitive to modulation by quin. Figure 2d shows a time course of $Ca_V1.3b$-β_3 current inhibition by Oxo-M whereas the time course with quin (Fig. 2e) shows no inhibition or kinetic change (Fig. 2e inset, g). Several concentrations of quin were tested but did not inhibit L-current to the same extent as Oxo-M (Fig. 2f). D_2Rs appeared to desensitize with 10 μM quin. Application of quin for 1 min to cells co-transfected with the D_2R-like family member, $D_{4.4}R$, inhibited L-current by 8.5 ± 2.5% and did not produce changes in TTP or *r*40 (Additional file 2).

To confirm that lack of L-current inhibition was not due to poor expression of D_2Rs, we repeated the experiment but substituted $Ca_V2.2$ for $Ca_V1.3b$ to serve as a positive control since activated D_2Rs also inhibit $Ca_V2.2$ [24–26]. Quin inhibited $Ca_V2.2$ by 45 ± 7% after 30 s and 48 ± 4% after 1 min (Fig. 3a). Inhibition occurred specifically by activating transfected D_2Rs because cells transfected without D_2Rs showed no response to quin (Fig. 3a, n = 3). Moreover, N-current inhibition by quin occurred in a concentration-dependent manner (Fig. 3b, n = 3–5). Compared to lower concentrations, 10 μM quin resulted in less inhibition; inhibited current did not recover upon wash, suggesting this concentration causes receptor desensitization (data not shown). Thus, our findings indicate that transfected D_2Rs functionally express in HEK-M1 cells to modulate $Ca_V2.2$, but not $Ca_V1.3b$ VGCC activity.

M_1R and D_2R pathways use different signaling mechanisms to inhibit N-current

To compare D_2Rs and M_1Rs signaling pathways on $Ca_V2.2$ current, we first confirmed that activation of the stably transfected M_1Rs could suppress N-current. Indeed, Oxo-M inhibited currents from β_3-containing channels by 70 ± 5% after 30 s (Fig. 3c). When incubated with the PLA_2 antagonist OPC, cells showed less N-current inhibition by Oxo-M, 14 ± 8% inhibition after 30 s (Fig. 3c). In contrast, low concentrations of quin still suppressed N-current in the presence of OPC (Fig. 3d). Inhibition was relieved by pre-pulse facilitation (Fig. 3e, g, h) and occurred in the presence of BSA, which acts as a scavenger of free AA (Fig. 3f–h), suggesting that quin mediates membrane-delimited inhibition of N-current. These findings suggest that M_1Rs and D_2Rs do not share a common pathway leading to N-current inhibition.

Discussion

Previously, the $Ca_V1.3b$ splice variant of L-VGCCs, found in MSNs, had not been specifically tested for modulation by GPCRs. Here, using HEK-M1 cells, we present the novel finding that M_1R stimulation inhibits $Ca_V1.3b$ L-current with the accessory $Ca_V\beta$-subunit determining the magnitude of inhibition. In contrast, stimulation of transfected D_2Rs with quin does not recapitulate L-current inhibition observed in MSNs [3]. Pharmacological sensitivity to both FPL and NIM confirmed that $Ca_V1.3b$ expressed in HEK-M1 cells behaves similarly to other recombinant $Ca_V1.3$ VGCCs [22, 27].

We also report that N-current modulation by the D_2R short splice variant appears similar to membrane-delimited inhibition by the D_2R long form [24]. In this form of modulation, when G proteins are activated, $G\beta\gamma$ directly binds to and inhibits $Ca_V2.2$ which can be reversed by strong prepulses [10, 28]. Indeed, D_2R-mediated inhibition of $Ca_V2.2$ was independent of PLA_2, whereas blockers of PLA_2 abolished inhibition by M_1Rs. Thus, the membrane-delimited pathway may be at least partially responsible for the inhibition of $Ca_V2.2$ by D_2Rs in MSNs [25].

In our experiments, the short splice variant of $Ca_V1.3$ ($Ca_V1.3b$) was unaffected by activation of D_2Rs, expressed in HEK-293 cells, similar to a previous report on $Ca_V1.3a$, which has a longer C-terminus [24]. Since neither D_2R-long inhibited $Ca_V1.3a$ [24], nor D_2R-short inhibited $Ca_V1.3b$ (Fig. 2f), one possibility is that another channel/receptor combination occurs in vivo; however, D_2R-long and short equally couple to G_i proteins [29]. On the other hand, $Ca_V1.3a$ binds a scaffolding protein found in the postsynaptic density of synapses known as Shank [30]. In MSNs, $Ca_V1.3a$ requires an association with Shank for current inhibition by D_2Rs [4]. Although lack of the longer

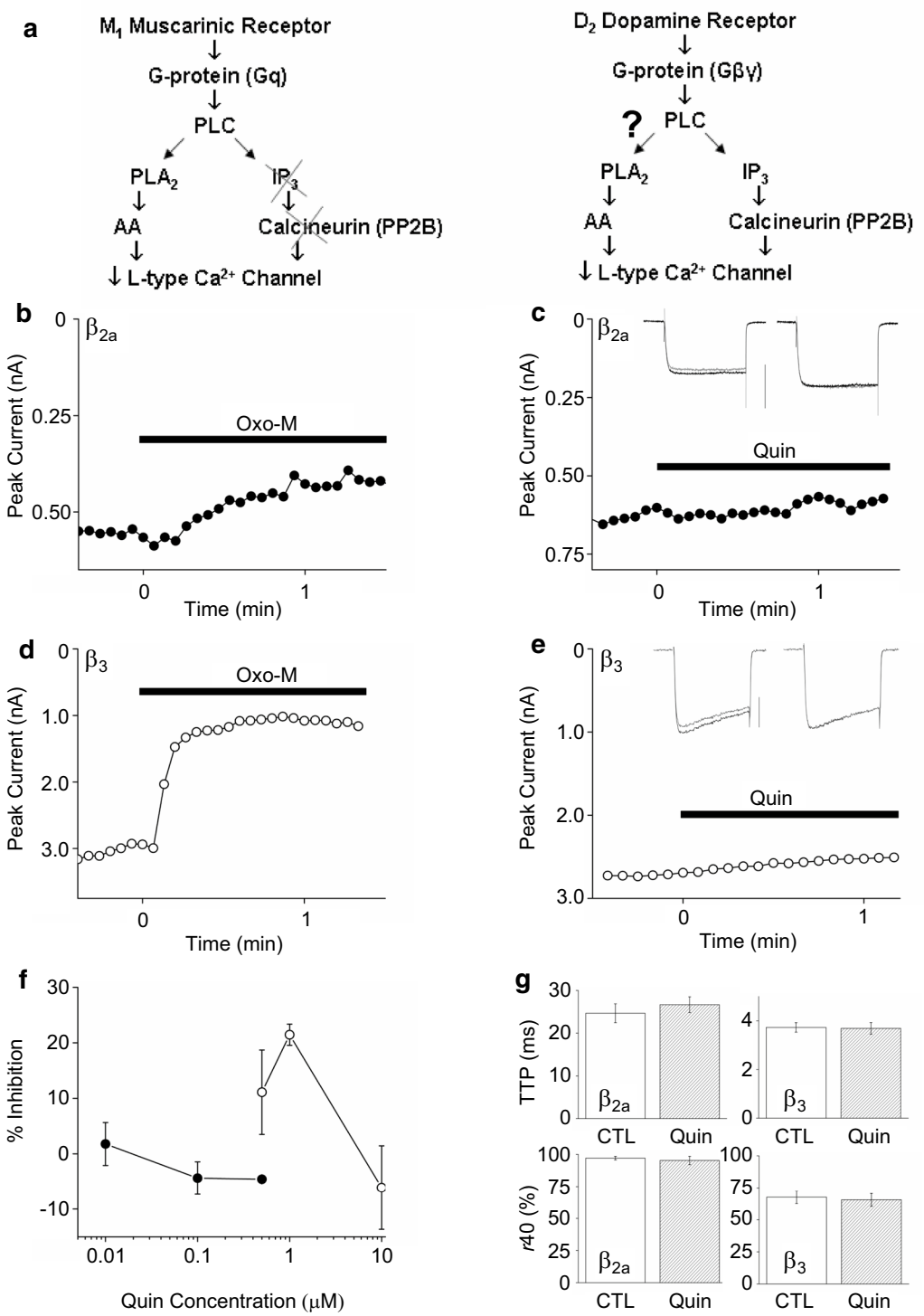

Fig. 2 M_1Rs but not D_2Rs inhibit recombinant L-current. **a** Comparison of M_1R and D_2R signaling pathways that inhibit L-VGCC activity. **b** Time course of Oxo-M applied at time 0 for $Ca_V1.3b$-β_{2a} current. **c** Time course of 10 nM quin applied at time 0 for $Ca_V1.3b$-β_{2a} current. Inset: (*left*) Individual current traces before (black) and after 1 min of quin, scale bar = 0.5 nA. (*right*) Normalized traces. **d** Time course of Oxo-M applied at time 0 for $Ca_V1.3b$-β_3 current. **e** Time course of 0.5 μM quin applied at time 0 for $Ca_V1.3b$-β_3 current. Inset: same as **c**, scale bar = 1 nA. **f** Concentration–response curve of quin on $Ca_V1.3b$-β_{2a} (filled circles) and $Ca_V1.3b$-β_3 (open circles) currents (n = 2–5). **g** Summary of kinetic analysis

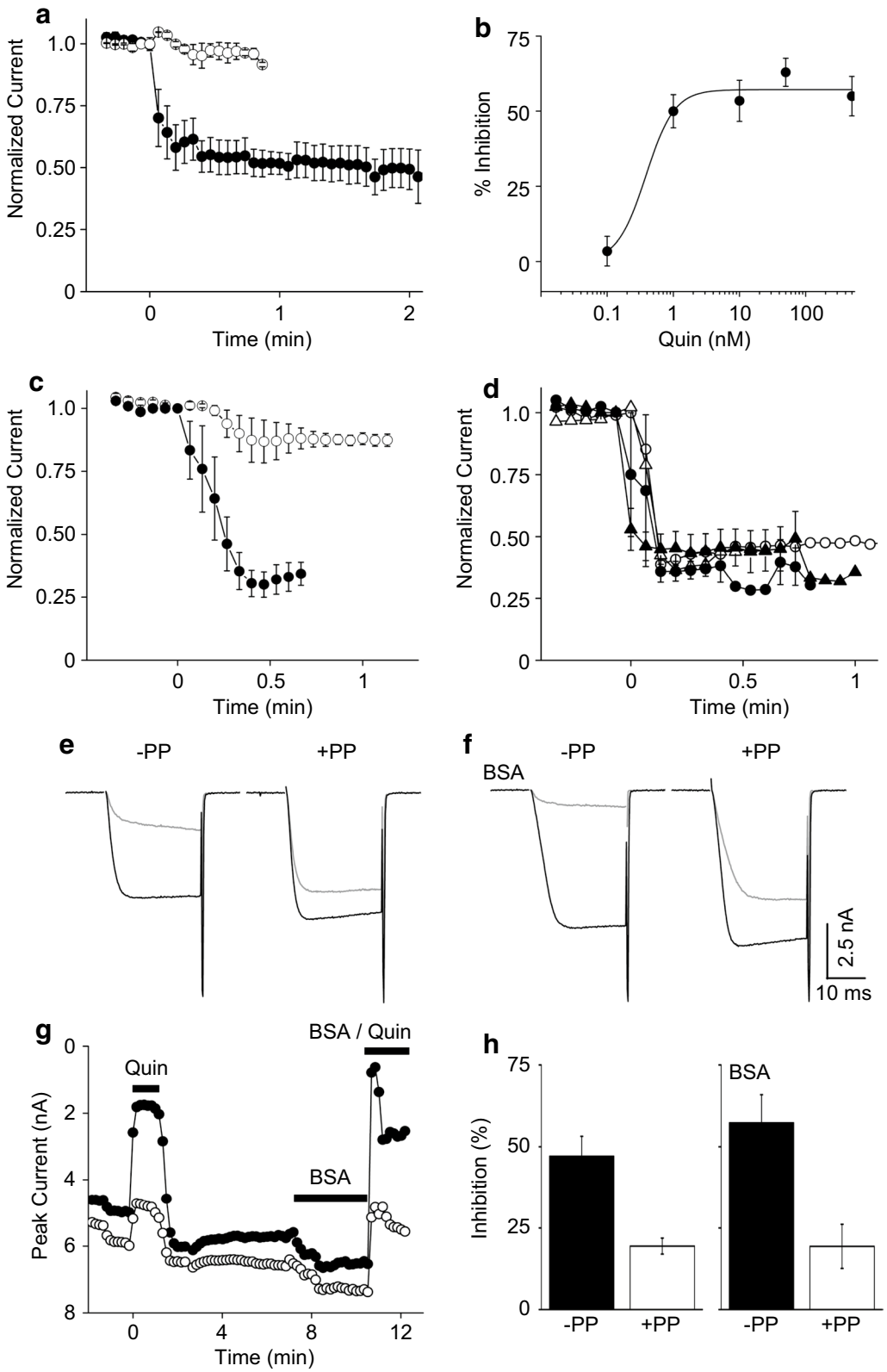
a
Normalized Current
1.0
0.75
0.50
0.25
0
0
1
2
Time (min)
b
% Inhibition
75
50
25
0
0.1
1
10
100
Quin (nM)
c
Normalized Current
1.0
0.75
0.50
0.25
0
0
0.5
1
Time (min)
d
Normalized Current
1.0
0.75
0.50
0.25
0
0
0.5
1
Time (min)
e
-PP
+PP
f
BSA
-PP
+PP
2.5 nA
10 ms
g
BSA / Quin
Quin
BSA
Peak Current (nA)
0
2
4
6
8
0
4
8
12
Time (min)
h
Inhibition (%)
75
50
25
0
BSA
-PP
+PP
-PP
+PP

(See figure on previous page.)
Fig. 3 D_2Rs and M_1Rs inhibit recombinant N-current demonstrating successful expression of both GPCRs. To demonstrate that D_2Rs are functional, HEK-M1 cells were transfected with the D_2R, $Ca_V2.2$, $\alpha_2\delta_1$, and a $Ca_V\beta$ subunit plasmids using the same conditions as described in the Methods section and in Additional file 1 legend as described for $Ca_V1.3b$. **a** Time course of $Ca_V2.2$-β_3 current inhibition by 0.5 μM quin added at time 0 with (filled circles, n = 8, $P < 0.001$ compared to CTL) or without (open circles, n = 3) co-transfection of D_2Rs. **b** Concentration–response curve of quin on $Ca_V2.2$-β_3 current (n = 3–5). **c** Time course of $Ca_V2.2$-β_3 current inhibition by Oxo-M added at time 0 under CTL conditions (filled circles, n = 5, $P < 0.001$ compared to CTL) or preincubation for at least 3 min with 10 μM of the PLA_2 antagonist, OPC (open circles, n = 5, $P < 0.05$ compared to Oxo-M alone, ANOVA). **d** Time course of $Ca_V2.2$-β_3 current inhibition by 10 (filled triangles) or 50 nM (filled circles) quin under control conditions or preincubated with OPC (open symbols) (n = 1–5). **e** Representative $Ca_V2.2$-β_{2a} currents measured at a test potential of + 20 mV (−PP) from a holding potential of − 90 mV. A 25 ms prepulse to + 120 mV was placed before a second test pulse (+PP) to measure for membrane-delimited inhibition. CTL current (black) or 30 s after application of 0.5 μM quin (grey). **f** Same as **e** in the presence of 1 mg/ml BSA. **g** Time course of $Ca_V2.2$-β_{2a} current (−PP, filled circles; +PP, open circles) exposed to 0.5 μM quin at time 0 for 1 min. After washing, current fully recovered; BSA was added for 3 min before addition of BSA/quin. **h** Summary of $Ca_V2.2$-β_{2a} inhibition by quin (n = 9) or BSA/quin (n = 3)

$Ca_V1.3$ C-terminus may explain the absence of channel modulation by D_2Rs in our studies, we found that Oxo-M inhibits $Ca_V1.3b$ currents, showing that this short splice variant of $Ca_V1.3$ can be modulated by a G_qPCR. Therefore, a missing intermediary protein vital for D_2R modulation of $Ca_V1.3b$ may underlie the lack of inhibition reported here, or D_2Rs may not modulate $Ca_V1.3b$.

Conclusions

These findings highlight the specific regulation of Ca^{2+} channels in a $Ca_V\beta$-subunit dependent manner by different neurotransmitters. While M_1R and D_2R pathways contain similar signaling molecules and share a common functional output of inhibiting Ca^{2+} channels, differences between the two cascades exist. Expression and localization of $Ca_V1.3b$ associated with different $Ca_V\beta$-subunits in a tissue or cell may dictate how Ca^{2+} influx is modulated by nearby GPCRs, ultimately affecting Ca^{2+}-dependent processes.

Limitations

Further experiments are needed to determine the differences in signaling between successful $Ca_V1.3b$ inhibition by M_1Rs versus none with D_2Rs.

Additional files

Additional file 1. Pharmacological characterization of $Ca_V1.3b$ L-current. HEK-M1 cells were washed with DMEM and the DNA mixture of $Ca_V1.3b$, $\alpha_2\delta$-1, a β_3-subunit and GFP was added and incubated for 1 h at 37 °C in a 5% CO_2 incubator. Supplemented media, without antibiotics, was then returned to the cells to bring the volume up to 1 ml (normal medium volume). After 2 h, cells were washed with supplemented media and washed a final time 2 h later. 10 mM $MgSO_4$ was added to the medium to block basal activity of $Ca_V1.3b$, which helped minimize excitotoxicity of transfected cells. Cells were transferred 24–72 h post-transfection using 2 mM EDTA in 1X PBS, to poly-*L*-lysine-coated coverslips. Recording began 1 h after transfer to coverslips. **A** Individual traces of $Ca_V1.3b$-β_3 current before (CTL) and after exposure to 0.3 μM NIM. **B** Concentration–response curve of L-current inhibition to NIM (n = 4–8). **C** $Ca_V1.3b$-β_{2a} currents before and after exposure to FPL (1 μM). Cells were stepped to a test potential of − 10 mV from a holding potential of − 90 mV followed by repolarization to − 90 or − 50 mV. Control (CTL) currents from β_{2a}-containing L-VGCCs show little to no inactivation as observed previously [31]. **D** $Ca_V1.3b$-β_3 currents before and after FPL. Cells were stepped to a test potential of − 10 mV from a holding potential of − 60 mV followed by repolarization to − 60 mV. Following FPL, both β_{2a}- and β_3-containing channels exhibited slower activation and deactivation kinetics, hallmarks of agonist action on L-current [32]. **E** FPL enhancement of the $Ca_V1.3b$-β_{2a} current–voltage plot from a holding potential of − 90 mV (CTL, filled circles; FPL, open circles, n = 3, $^*P < 0.05$). **F** Concentration–response curve of $Ca_V1.3b$-β_3 tail current enhancement to FPL (n = 4–8). Currents inhibited by NIM and enhanced by FPL fully recovered by washing with bath solution (data not shown).

Additional file 2. $D_{4.4}$Rs do not inhibit recombinant L-current. **A** Summary bar graph of $Ca_V1.3b$-β_3 current inhibition by 0.5 μM quin (n = 5). **B & C** Summary bar graphs of TTP and *r*40 kinetic analysis.

Abbreviations

AA: arachidonic acid; $cPLA_2$: Ca^{2+} dependent, cytosolic phospholipase A_2; D_2Rs: dopaminergic D_2 receptors; FPL: FPL 64176; GFP: green fluorescent protein; GPCRs: G protein-coupled receptors; HEK-293 cells: human embryonic kidney cells; M_1Rs: muscarinic M_1 receptors; MSN: medium spiny neurons; NIM: nimodipine; NMG: N-methyl-*D*-glucamine; OPC: oleoyloxyethyl phosphorylcholine; Oxo-M: Oxotremorine-M; PLA_2: phospholipase A_2; PLC: phospholipase C; PTX: pertussis toxin; Quin: quinpirole; SCG: superior cervical ganglion; TTP: time to peak; VGCCs: voltage-gated Ca^{2+} channels.

Authors' contributions

MLR conceived of the project, experimental design, collected and analyzed data, and wrote the manuscript. ARR contributed to the experimental design, analysis and editing of the manuscript. Both authors read and approved the final manuscript.

Author details

[1] Department of Physiology, Program in Neuroscience, University of Massachusetts Medical School, 55 Lake Ave North, Worcester, MA 01655, USA. [2] Department of Microbiology and Physiological Systems, Program in Neuroscience, University of Massachusetts Medical School, 368 Plantation Street, Worcester, MA 01605, USA.

Acknowledgements

We thank José Lemos, Elizabeth Luna, Haley Melikian, Tora Mitra-Ganguli and Edward Perez-Reyes for their feedback.

Competing interests

The authors declare that they have no competing interests.

Availability of data and materials

The accession numbers for the constructs used in this study are as follows: $Ca_V1.3b$ (+exon11, Δexon32, +exon42a), GenBank accession #AF370009; $Ca_V2.2$ ([a]10, Δexon18a, Δexon24a, +exon31a, +exon37b, +exon46), GenBank

accession #AF055477; $Ca_V\beta_{1b}$, GenBank accession #X61394; $Ca_V\beta_{2a}$, GenBank accession #M80545; $Ca_V\beta_3$, GenBank accession #M88751; $Ca_V\beta_4$, GenBank accession #L02315; and $\alpha_2\delta$-1, GenBank accession #AF286488. All data generated or analyzed during this study are included in this published article (and its additional files).

Consent for publication
Not relevant.

Ethics approval and consent to participate
Not applicable.

Funding
Salary support to Mandy Roberts-Crowley from NIH Kirschstein NRSA (5 TS32 NS07366-09). Research supplies and salary support (ARR) were supplied by AHA (9940225N), NIH (R01-NS34195), and from the University of Massachusetts Medical School.

Publisher's Note

Received: 31 July 2018 Accepted: 20 September 2018
Published online: 27 September 2018

References

1. Catterall WA, Perez-Reyes E, Snutch TP, Striessnig J. International Union of Pharmacology. XLVIII. Nomenclature and structure-function relationships of voltage-gated calcium channels. Pharmacol Rev. 2005;57(4):411–25.
2. Howe AR, Surmeier DJ. Muscarinic receptors modulate N-, P-, and L-type Ca^{2+} currents in rat striatal neurons through parallel pathways. J Neurosci. 1995;15(1 Pt 1):458–69.
3. Hernandez-Lopez S, Tkatch T, Perez-Garci E, Galarraga E, Bargas J, Hamm H, Surmeier DJ. D2 dopamine receptors in striatal medium spiny neurons reduce L-type Ca^{2+} currents and excitability via a novel PLC[beta]1-IP3-calcineurin-signaling cascade. J Neurosci. 2000;20(24):8987–95.
4. Olson PA, Tkatch T, Hernandez-Lopez S, Ulrich S, Ilijic E, Mugnaini E, Zhang H, Bezprozvanny I, Surmeier DJ. G-protein-coupled receptor modulation of striatal $Ca_V1.3$ L-type Ca^{2+} channels is dependent on a Shank-binding domain. J Neurosci. 2005;25(5):1050–62.
5. Stanika RI, Flucher BE, Obermair GJ. Regulation of postsynaptic stability by the L-type calcium channel $Ca_V1.3$ and its interaction with PDZ proteins. Curr Mol Pharmacol. 2015;8(1):95–101.
6. Berger SM, Bartsch D. The role of L-type voltage-gated calcium channels Cav1.2 and Cav1.3 in normal and pathological brain function. Cell Tissue Res. 2014;357(2):463–76.
7. Haley JE, Delmas P, Offermanns S, Abogadie FC, Simon MI, Buckley NJ, Brown DA. Muscarinic inhibition of calcium current and M current in Galpha q-deficient mice. J Neurosci. 2000;20(11):3973–9.
8. Shapiro MS, Loose MD, Hamilton SE, Nathanson NM, Gomeza J, Wess J, Hille B. Assignment of muscarinic receptor subtypes mediating G-protein modulation of Ca^{2+} channels by using knockout mice. Proc Natl Acad Sci USA. 1999;96(19):10899–904.
9. Liu L, Rittenhouse AR. Arachidonic acid mediates muscarinic inhibition and enhancement of N-type Ca^{2+} current in sympathetic neurons. Proc Natl Acad Sci USA. 2003;100(1):295–300.
10. Hille B. Modulation of ion-channel function by G-protein-coupled receptors. Trends Neurosci. 1994;17(12):531–6.
11. Liu L, Barrett CF, Rittenhouse AR. Arachidonic acid both inhibits and enhances whole cell calcium currents in rat sympathetic neurons. Am J Physiol Cell Physiol. 2001;280(5):C1293–305.
12. Liu L, Rittenhouse AR. Effects of arachidonic acid on unitary calcium currents in rat sympathetic neurons. J Physiol. 2000;525(Pt 2):391–404.
13. Roberts-Crowley ML, Rittenhouse AR. Arachidonic acid inhibition of L-type calcium ($Ca_V1.3b$) channels varies with accessory Ca_Vbeta subunits. J Gen Physiol. 2009;133(4):387–403.
14. Lin Z, Harris C, Lipscombe D. The molecular identity of Ca channel alpha 1-subunits expressed in rat sympathetic neurons. J Mol Neurosci. 1996;7(4):257–67.
15. Liu L, Roberts ML, Rittenhouse AR. Phospholipid metabolism is required for M_1 muscarinic inhibition of N-type calcium current in sympathetic neurons. Eur Biophys J EBJ. 2004;33(3):255–64.
16. Liu L, Zhao R, Bai Y, Stanish LF, Evans JE, Sanderson MJ, Bonventre JV, Rittenhouse AR. M_1 muscarinic receptors inhibit L-type Ca^{2+} current and M-current by divergent signal transduction cascades. J Neurosci. 2006;26(45):11588–98.
17. Tence M, Cordier J, Premont J, Glowinski J. Muscarinic cholinergic agonists stimulate arachidonic acid release from mouse striatal neurons in primary culture. J Pharmacol Exp Ther. 1994;269(2):646–53.
18. Bhattacharjee AK, Chang L, Lee HJ, Bazinet RP, Seemann R, Rapoport SI. D2 but not D1 dopamine receptor stimulation augments brain signaling involving arachidonic acid in unanesthetized rats. Psychopharmacology. 2005;180(4):735–42.
19. Felder CC, Kanterman RY, Ma AL, Axelrod J. A transfected m1 muscarinic acetylcholine receptor stimulates adenylate cyclase via phosphatidylinositol hydrolysis. J Biol Chem. 1989;264(34):20356–62.
20. Nilsson CL, Hellstrand M, Ekman A, Eriksson E. Direct dopamine D_2-receptor-mediated modulation of arachidonic acid release in transfected CHO cells without the concomitant administration of a Ca^{2+}-mobilizing agent. Br J Pharmacol. 1998;124(8):1651–8.
21. Peralta EG, Ashkenazi A, Winslow JW, Smith DH, Ramachandran J, Capon DJ. Distinct primary structures, ligand-binding properties and tissue-specific expression of four human muscarinic acetylcholine receptors. EMBO J. 1987;6(13):3923–9.
22. Xu W, Lipscombe D. Neuronal Ca(V)1.3alpha(1) L-type channels activate at relatively hyperpolarized membrane potentials and are incompletely inhibited by dihydropyridines. J Neurosci. 2001;21(16):5944–51.
23. Hell JW, Westenbroek RE, Warner C, Ahlijanian MK, Prystay W, Gilbert MM, Snutch TP, Catterall WA. Identification and differential subcellular localization of the neuronal class C and class D L-type calcium channel alpha 1 subunits. J Cell Biol. 1993;123(4):949–62.
24. Bell DC, Butcher AJ, Berrow NS, Page KM, Brust PF, Nesterova A, Stauderman KA, Seabrook GR, Nurnberg B, Dolphin AC. Biophysical properties, pharmacology, and modulation of human, neuronal L-type (alpha(1D), Ca(V)1.3) voltage-dependent calcium currents. J Neurophysiol. 2001;85(2):816–27.
25. Yan Z, Song WJ, Surmeier J. D_2 dopamine receptors reduce N-type Ca^{2+} currents in rat neostriatal cholinergic interneurons through a membrane-delimited, protein-kinase-C-insensitive pathway. J Neurophysiol. 1997;77(2):1003–15.
26. Leroy J, Richards MW, Butcher AJ, Nieto-Rostro M, Pratt WS, Davies A, Dolphin AC. Interaction via a key tryptophan in the I-II linker of N-type calcium channels is required for beta1 but not for palmitoylated beta2, implicating an additional binding site in the regulation of channel voltage-dependent properties. J Neurosci. 2005;25(30):6984–96.
27. Safa P, Boulter J, Hales TG. Functional properties of Cav1.3 (alpha1D) L-type Ca^{2+} channel splice variants expressed by rat brain and neuroendocrine GH3 cells. J Biol Chem. 2001;276(42):38727–37.
28. Bernheim L, Beech DJ, Hille B. A diffusible second messenger mediates one of the pathways coupling receptors to calcium channels in rat sympathetic neurons. Neuron. 1991;6(6):859–67.
29. Senogles SE. The D2 dopamine receptor isoforms signal through distinct G_i alpha proteins to inhibit adenylyl cyclase. A study with site-directed mutant G_i alpha proteins. J Biol Chem. 1994;269(37):23120–7.
30. Zhang H, Maximov A, Fu Y, Xu F, Tang TS, Tkatch T, Surmeier DJ, Bezprozvanny I. Association of $Ca_V1.3$ L-type calcium channels with Shank. J Neurosci. 2005;25(5):1037–49.
31. Chien AJ, Carr KM, Shirokov RE, Rios E, Hosey MM. Identification of palmitoylation sites within the L-type calcium channel beta2a subunit and effects on channel function. J Biol Chem. 1996;271(43):26465–8.
32. Rampe D, Lacerda AE. A new site for the activation of cardiac calcium channels defined by the nondihydropyridine FPL 64176. J Pharmacol Exp Ther. 1991;259(3):982–7.